Research Article

Xiaoyu Zha#, Gaowen Li#, Ling Zhang, Qun Chen, Qing Xia*

Identification of active compounds in Ophiopogonis Radix from different geographical origins by UPLC-Q/TOF-MS combined with GC-MS approaches

https://doi.org/10.1515/biol-2022-0096
received December 15, 2021; accepted May 09, 2022

Abstract: Ophiopogonis Radix, also known as Maidong in Chinese, is largely produced in the Sichuan and Zhejiang provinces: "Chuan-maidong (CMD)" and "Zhe-maidong (ZMD)," respectively. This study aimed to distinguish and evaluate the quality of CMD and ZMD. In this study, the tubers of CMD and ZMD were investigated using UPLC-Q/TOF-MS, GC-MS, and LC-MS methods, respectively. Overall, steroidal saponins, homoisoflavonoids, amino acids, and nucleosides were quickly identified. Furthermore, multivariate statistical analysis revealed that CMD and ZMD could be separated. Moreover, CMD showed higher levels of 4-aminobutanoic acid, glycine, L-proline, monoethanolamine, and serine than ZMD. Besides, the levels of chlorogenic acid, traumatic acid, cytidine, cadaverine, pyridoxine 5-phosphate, glutinone, and pelargonidin 3-*O*-(6-*O*-malonyl-β-D-glucoside) were remarkably higher in ZMD than in CMD. Furthermore, these different constituents were mainly associated with galactose metabolism; starch and sucrose metabolism; cysteine and methionine metabolism; valine, leucine, and isoleucine biosynthesis; and glycerophospholipid metabolism. In general, these results showed many differences between the bioactive chemical constituents of *Ophiopogon japonicus* from different production areas, where ZMD performed better in the quality assessment than CMD, and that UPLC-Q/TOF-MS, GC-MS, and LC-MS are effective methods to discriminate medicinal herbs from different production areas.

Keywords: Ophiopogonis Radix, Maidong, UPLC-Q/TOF-MS, GC-MS, LC-MS

1 Introduction

Ophiopogonis Radix (known as Maidong), the root tuber of *Ophiopogon japonicus* Ker-Gawl, belongs to the family Liliaceae and is the most widely used traditional Chinese medicine (TCM) in the Chinese Pharmacopoeia [1]. According to TCM theory, Maidong nourishes yin, moistens the lungs, promotes body fluid production, eases the mind, and clears away heart fires [2,3]. It has been employed to control diabetes and its complications [4], radiation pneumonitis [5], atherosclerotic coronary heart disease, and viral myocarditis [6]. Additionally, modern phytochemical studies have suggested that Maidong is rich in various biologically active compounds, including steroidal saponins, amino acids, homoisoflavonoids, polysaccharides, and nucleosides, which have beneficial immunomodulatory, anti-inflammatory, central nervous system protective, antioxidative, and anti-apoptosis effects [7–9]. Although several studies on the chemical components of Maidong have been reported, these studies were performed with a single analytical technique and are not comprehensive [10,11]. Therefore, to the best of our knowledge, there is still a lack of information on the comprehensive chemical constituents of Maidong determined by using a multidimensional assessment approach.

At present, the cultivation regions of Ophiopogonis Radix are mainly concentrated in the Sichuan (mainly Santai County) and Zhejiang provinces (mainly the city of Cixi) of China. Ophiopogonis Radix from Sichuan and Zhejiang provinces is popularly called Chuan-maidong (CMD) and Zhe-maidong (ZMD), respectively, but ZMD is generally considered superior to Ophiopogonis Radix

# These authors contributed equally to this work.

*** Corresponding author: Qing Xia,** Department of Pharmacology, Ningbo College of Health Science, Rd. Xuefu 51#, Yinzhou District, 315100 Ningbo, Zhejiang, China, e-mail: sunnyxq@zju.edu.cn
Xiaoyu Zha, Gaowen Li, Ling Zhang, Qun Chen: Department of Pharmacology, Ningbo College of Health Science, Rd. Xuefu 51#, Yinzhou District, 315100 Ningbo, Zhejiang, China

cultivated in other provinces [10]. Currently, it is generally accepted that the quantity and pharmacological effects of tubers on Maidong in different areas are controlled by environmental conditions and endogenous factors [11]. A study by Lu et al. found that the chemical constituents of CMD and ZMD differed much from each other according to high-performance liquid chromatography-mass spectrometry (LC-MS) with multivariate statistical analysis [12]. With the structural transformation of economic development, the cultivation of ZMD has drastically decreased in Zhejiang Province in recent years. Sichuan has now become the primary place of MD production [10,12]. In addition, CMD and ZMD are difficult to distinguish based on their appearance, which has also made quality control of Maidong challenging. Considering these findings, further study of the compositional distinction between Maidong tubers grown in Sichuan and Zhejiang provinces remains limited. Differences between the chemical constituents of CMD and ZMD have been reported by using LC coupled with evaporative light scattering detection, gas chromatography (GC) coupled with MS, or LC coupled with MS [2,10,13]. Because of the complexity of chemical constituents, those studies only assessed saponins, polysaccharides, or homoisoflavonoids.

Thus, this study aimed to comprehensively characterize the bioactive constituents of CMD and ZMD from the two producing areas and investigate their metabolic pathway. In this study, CMD and ZMD tubers were collected, and the chemical information of multiple bioactive constituents was characterized by using ultra-performance liquid chromatography-quadrupole-time-of-flight mass spectrometry (UPLC-Q/TOF-MS), as well as GC-MS and LC-MS methods with multivariate statistical analysis, including principal component analysis (PCA) and orthogonal partial least squares-discriminate analysis (OPLS-DA). Furthermore, the pathways of significantly different chemical constituents were identified to reveal the potential biological events occurring between CMD and ZMD.

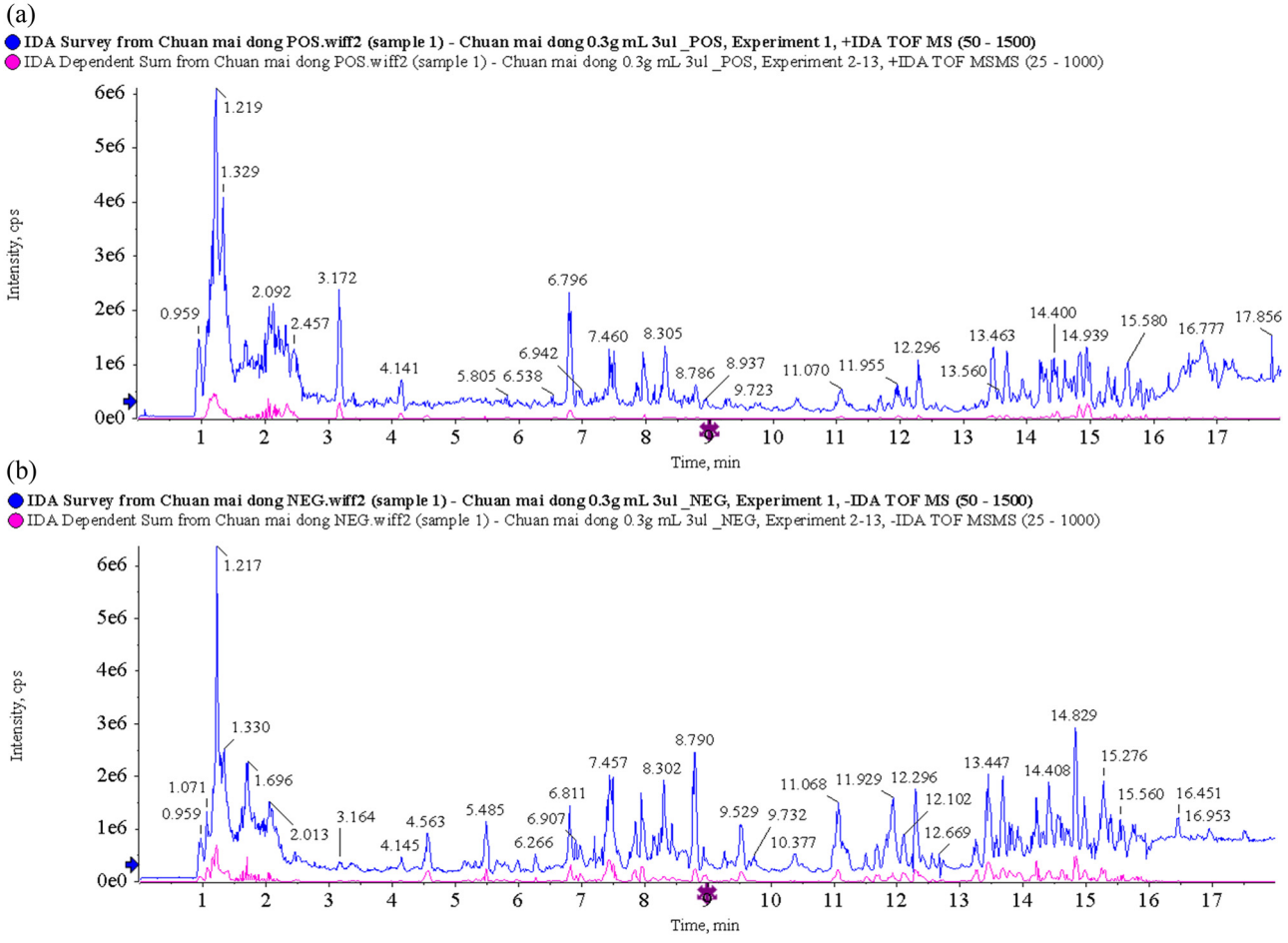

Figure 1: Total ion chromatogram of CMD obtained by UPLC/Q-TOF MS analysis in (a) positive ion mode and (b) negative ion mode.

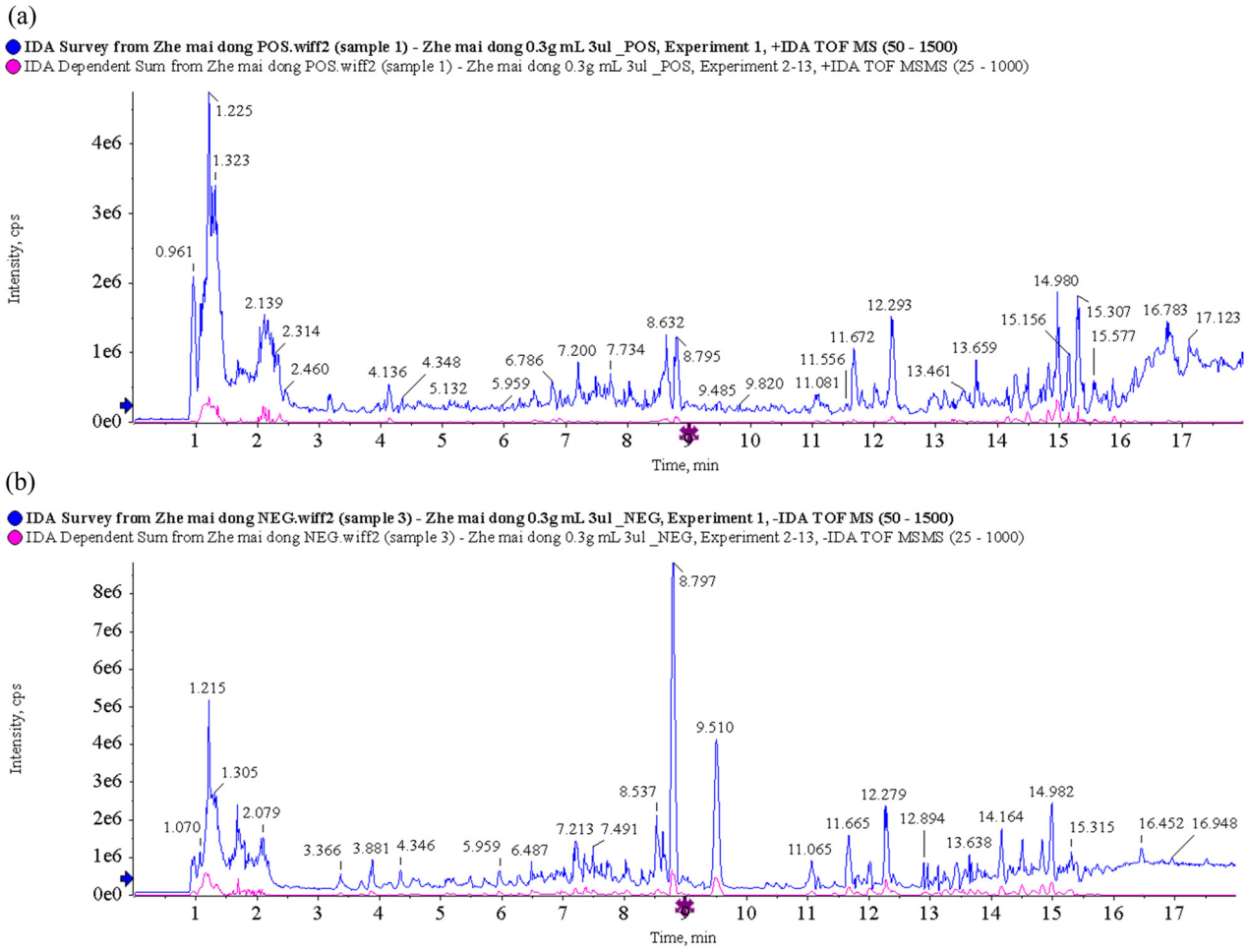

Figure 2: Total ion chromatogram of ZMD obtained by UPLC/Q-TOF MS analysis in (a) positive ion mode and (b) negative ion mode.

Therefore, the results of this study might provide a guide for a comprehensive evaluation and quality control, as well as a study on the mechanism of Ophiopogonis Radix.

2 Materials and methods

2.1 Chemicals and reagents

Ultrapure water was prepared by a Milli-Q system (Milford, MA, USA). Acetonitrile and methanol (HPLC grade) were produced by Merck (Darmstadt, Germany). Bis(trimethylsilyl)trifluoroacetamide was obtained from CNW Technologies (Shanghai, China). DL-*o*-Chlorophenylalanine was purchased from GL Biochem (Shanghai) Ltd (Shanghai, China). All the other chemicals and solvents were of analytical grade (purity (S98%) for GC/LC use.

2.2 Plant materials

CMD and ZMD at the same growth stage were collected from the market as mature plants in the cities of Cixi (Zhejiang, China) and Mianyang (Sichuan, China) in May 2020, respectively, including six batches of ZMD and six batches of CMD samples. All the samples were authenticated by Professor Qing Xia, Ningbo College of Health & Science, Ningbo, Zhejiang, China.

2.3 Sample preparation for UPLC-Q/TOF-MS analysis

The aim of the present study was to thoroughly evaluate the polysaccharides and saponins of CMD and ZMD in water extract solutions. Briefly, the dried tubers of CMD and ZMD were ground and passed through a standard

Table 1: Putative identification of CMD in positive ion mode

No.	Component name	Area	RT	Formula	Precursor mass	Found at mass	Mass error (ppm)
1	L(+)-Arginine	7,402,000	1.14	$C_6H_{14}N_4O_2$	175.119	175.1187	−1.5
2	Trigonelline	253,900	1.21	$C_7H_7NO_2$	138.055	138.0551	1
3	Proline	433,800	1.24	$C_5H_9NO_2$	116.071	116.0707	0.4
4	Glutamic acid	187,400	1.3	$C_5H_9NO_4$	148.06	148.0606	0.8
5	Betaine	140,700	1.37	$C_5H_{11}NO_2$	118.086	118.0863	0.6
6	Nicotinic acid	155,300	1.71	$C_6H_5NO_2$	124.039	124.0394	0.9
7	Nicotinamide	235,400	1.79	$C_6H_6N_2O$	123.055	123.0554	0.9
8	Adenosine	2,131,000	2.36	$C_{10}H_{13}N_5O_4$	268.104	268.1038	−0.9
9	Cordycepin	43,090	2.42	$C_{10}H_{13}N_5O_3$	252.109	252.1093	0.8
10	Guanosine	207,900	2.46	$C_{10}H_{13}N_5O_5$	284.099	284.0992	0.7
11	Phenylalanine	1,719,000	3.17	$C_9H_{11}NO_2$	166.086	166.0863	0.3
12	Cinnamic acid	48,090	3.18	$C_9H_8O_2$	149.06	149.0598	0.6
13	4-Hydroxybenzoic acid	12,960	4.73	$C_7H_6O_3$	139.039	139.039	0.4
14	Esculetin	23,820	5.13	$C_9H_6O_4$	179.034	179.034	0.6
15	Hyperin	4,621	6.5	$C_{21}H_{20}O_{12}$	465.103	465.1034	1.4
16	Syringaldehyde	3,442	6.56	$C_9H_{10}O_4$	183.065	183.065	−1.1
17	Luteoloside	2,638	6.67	$C_{21}H_{20}O_{11}$	449.108	449.1091	2.8
18	Isoferulic acid	3,834	6.74	$C_{10}H_{10}O_4$	195.065	195.0652	0.1
19	Narirutin	2,831	7.08	$C_{27}H_{32}O_{14}$	581.186	581.1873	1.4
20	Neohesperidin	4,766	7.5	$C_{28}H_{34}O_{15}$	611.197	611.1977	1.1
21	Tiliroside	4,904	8.91	$C_{30}H_{26}O_{13}$	595.145	595.145	0.7
22	Calycosin-7-*O*-glucoside	6,176	9.42	$C_{22}H_{22}O_{10}$	447.129	447.1284	−0.4
23	Nobiletin	31,320	12.77	$C_{21}H_{22}O_8$	403.139	403.1388	0.1
24	Ophiopogonin D′	877,800	14.83	$C_{44}H_{70}O_{16}$	855.474	855.4731	−0.6
25	Ruscogenin	178,800	14.85	$C_{27}H_{42}O_4$	431.316	431.3154	−0.5
26	Ophiopogonanone C	3,902	15.06	$C_{20}H_{20}O_6$	357.133	357.134	1.9

60-mesh filter. The obtained powder (3.0 g) was accurately weighed into a conical flask, immersed in 200 mL of distilled water for 30 min, and boiled for 90 min. Then, the liquid extract obtained was concentrated to 10 g by using rotating evaporation (JC-ZF-1L, Qingdao Juchuang Times Environmental Protection Technology Co., Ltd, China). The obtained liquid extract was dissolved in methanol at a weight ratio of 1:1 and centrifuged at a speed of 14,000 rpm for 20 min before UPLC-Q/TOF-MS analysis.

2.4 Sample preparation for GC-MS analysis

Additionally, approximately 50 mg of the dried tubers of CMD and ZMD were used for the extraction procedure. Briefly, CMD and ZMD were mixed with 800 µL of methanol containing an internal standard (2.8 mg/mL DL-*o*-Chlorophenylalanine). Then, all samples were ground to a fine powder using a grinding mill operated at 65 Hz for 120 s. The samples were ultrasonicated at 4 kHz in an ice bath for 30 min and then centrifuged at 12,000 rpm at 4°C for 10 min. Subsequently, 200 µL of the supernatant was evaporated to dryness at room temperature. After that, the samples were derivatized by shaking with 30 µL of methoxyamine hydrochloride (20 mg/mL) in pyridine for 90 min at 37°C. The samples were then trimethylsilylated by adding 30 µL of bis(trimethylsilyl)trifluoroacetamide and incubated for 1 h at 70°C. After the reaction was complete, the samples were incubated for 1 h at room temperature. Finally, 200 µL of the supernatant was transferred to a vial for GC-MS analysis. The mix of all extract solutions was used as a control sample (QC).

2.5 Sample preparation for LC-MS analysis

Furthermore, approximately 50 mg of the dried tubers of CMD and ZMD were applied for the extraction procedure. Briefly, CMD and ZMD were extracted with 800 µL of methanol containing DL-*o*-Chlorophenylalanine (2.8 mg/mL) to investigate flavonoids. All samples were ground to a fine powder using a grinding mill operated at 65 Hz for 120 s. The samples were ultrasonicated at 40 kHz in an ice bath for 30 min and then centrifuged at 12,000 rpm at 4°C for 15 min. After that, 200 µL of the supernatant was transferred to a vial for LC-MS analysis. The mix of all extract solutions was used as QC.

Table 2: Putative identification of CMD in negative ion mode

No.	Component name	Area	RT	Formula	Precursor mass	Found at mass	Mass error (ppm)
1	Histidine	17,540	1.09	$C_6H_9N_3O_2$	154.062	154.0621	−0.7
2	L(+)-Arginine	165,100	1.1	$C_6H_{14}N_4O_2$	173.104	173.1044	0.2
3	Glutamic acid	57,600	1.14	$C_5H_9NO_4$	146.046	146.046	0.6
4	D-(+)-Mannose	786,300	1.22	$C_6H_{12}O_6$	179.056	179.0562	0.4
5	L-Malic acid	3,632,000	1.38	$C_4H_6O_5$	133.014	133.0144	0.9
6	Citric acid	9,523,000	1.9	$C_6H_8O_7$	191.02	191.0198	0.3
7	Succinic acid	58,120	2.29	$C_4H_6O_4$	117.019	117.0193	0
8	Leucine	473,700	2.47	$C_6H_{13}NO_2$	130.087	130.0873	0
9	Guanosine	335,800	2.47	$C_{10}H_{13}N_5O_5$	282.084	282.0844	0.1
10	Gallic acid	10,950	2.65	$C_7H_6O_5$	169.014	169.0142	−0.3
11	Phenylalanine	592,600	3.18	$C_9H_{11}NO_2$	164.072	164.0717	−0.1
12	Vanillic acid	119,600	3.37	$C_8H_8O_4$	167.035	167.035	0.2
13	L-Tryptophan	383,500	4.16	$C_{11}H_{12}N_2O_2$	203.083	203.0827	0.7
14	4-Hydroxybenzoic acid	36,400	4.63	$C_7H_6O_3$	137.024	137.0245	0.9
15	4-*O*-caffeoyl quinic acid	21,560	4.8	$C_{16}H_{18}O_9$	353.088	353.0881	0.8
16	Esculetin	151,700	5.13	$C_9H_6O_4$	177.019	177.0195	0.8
17	Caffeic acid	154,600	5.21	$C_9H_8O_4$	179.035	179.0351	0.6
18	Shikimic acid	548,900	5.49	$C_7H_{10}O_5$	173.046	173.0454	−0.9
19	Ellagic acid	28,660	6.35	$C_{14}H_6O_8$	300.999	300.999	0.1
20	Hyperin	34,590	6.51	$C_{21}H_{20}O_{12}$	463.088	463.0875	−1.4
21	Narirutin	8,615	7.08	$C_{27}H_{32}O_{14}$	579.172	579.1718	−0.3
22	Neohesperidin	16,980	7.5	$C_{28}H_{34}O_{15}$	609.182	609.1827	0.4
23	Tiliroside	16,580	8.92	$C_{30}H_{26}O_{13}$	593.13	593.1292	−1.4
24	Calycosin-7-*o*-glucoside	4,825	9.43	$C_{22}H_{22}O_{10}$	491.119	491.1188	−1.4
25	Gracillin	14,970	10.78	$C_{45}H_{72}O_{17}$	929.475	929.473	−2.3
26	Liriope muscari baily saponins C	165,000	13.46	$C_{44}H_{70}O_{17}$	869.454	869.4514	−3
27	Methylophiopogonone A	386,000	14.71	$C_{19}H_{16}O_6$	339.087	339.0864	−2.9
28	Ophiopogonin D	3,242,000	14.83	$C_{44}H_{70}O_{16}$	899.465	899.4623	−2.6
29	Methylophiopogonanone B	2,266,000	14.99	$C_{19}H_{20}O_5$	327.124	327.1228	−3
30	Liriopesides B	181,500	15.12	$C_{39}H_{62}O_{12}$	767.422	767.4199	−3.1
31	Gingerglycolipid B	5,459	15.2	$C_{33}H_{58}O_{14}$	723.381	723.3788	−2.8
32	Corosolic acid	3,440	15.55	$C_{30}H_{48}O_4$	471.348	471.3459	−4.4
33	Ophiopogonanone C	75,350	15.72	$C_{19}H_{16}O_7$	355.082	355.0814	−2.7

2.6 UPLC-Q/TOF-MS analysis and MS conditions

UPLC-Q/TOF-MS analysis was performed on a Waters ACQUITY UPLC I-Class PLUS system (Waters Corporation, Milford, MA, USA) coupled with hybrid quadrupole time-of-flight tandem mass spectrometer (SCIEX X-500R, SCIEX, Framingham, MA, USA) equipped with TurboIonSpray sources and a Turbo ion spray interface. Briefly, chromatographic separation was performed on a Waters UPLC BEH C_{18} column (100 mm × 2.1 mm, 1.7 μm particle size) at 40°C with a flow rate of 0.3 mL/min, and the injection volume was 3 μL. The mobile phase was composed of 0.1% ammonium formate in acetonitrile (A) and 0.1% formic acid aqueous solution (B) and introduced under the following gradient conditions: 0–12 min, 99% A–50% A; 12–14.5 min, 50–15% A; 14.5–15 min, 15–1% A; 15–18 min, 1% A; 18–18.1 min, 1% B–99% A; and 18.1–21 min, 99% A. TOF MS was performed using a Turbo Ion Spray ion source and ESI positive (+) and negative (−) ion scanning modes. The MS analysis conditions were as follows: source temperature: 600°C; nebulizing gas (N_2): 55 psi; drying gas (N_2): 45 psi; curtain gas (CUR): 35 psi; IonSpray Voltage Floating: 5,500 V/−4,500 V; TOF MS scan m/z range: 100–1,500 Da; TOF-MS/MS scan m/z range: 25–1,500 Da; TOF MS scan accumulation time: 0.25 s/spectra; and product ion scan accumulation time: 0.035 s/spectra. MS uses information-dependent acquisition and high sensitivity mode.

2.7 GC-MS analysis

An Agilent 6890A/5973C GC-MS system and a DB-5MS fused-silica capillary column (30 m × 0.25 mm × 0.25 μm, Agilent J&W Scientific, USA) were used for analysis. The injector

Table 3: Putative identification of ZMD in positive ion mode

No.	Component name	Area	RT	Formula	Precursor mass	Found at mass	Mass error (ppm)
1	L(+)-Arginine	4,301,000	1.11	$C_6H_{14}N_4O_2$	175.119	175.1189	−0.5
2	Trigonelline	207,100	1.2	$C_7H_7NO_2$	138.055	138.0551	1.2
3	Proline	2,757,000	1.22	$C_5H_9NO_2$	116.071	116.0706	0
4	Nicotinic acid	56,410	1.72	$C_6H_5NO_2$	124.039	124.0395	1.6
5	Nicotinamide	208,200	1.8	$C_6H_6N_2O$	123.055	123.0553	0.4
6	Adenosine	926,700	2.35	$C_{10}H_{13}N_5O_4$	268.104	268.104	−0.2
7	Cordycepin	41,280	2.42	$C_{10}H_{13}N_5O_3$	252.109	252.1096	1.9
8	Isoleucine	280,500	2.46	$C_6H_{13}NO_2$	132.102	132.1019	−0.2
9	Guanosine	90,750	2.47	$C_{10}H_{13}N_5O_5$	284.099	284.0995	1.9
10	Phenylalanine	285,000	3.17	$C_9H_{11}NO_2$	166.086	166.0863	0.4
11	Chlorogenic acid	57,310	4.64	$C_{16}H_{18}O_9$	355.102	355.1031	2
12	4-Hydroxybenzoic acid	14,360	4.73	$C_7H_6O_3$	139.039	139.0391	0.9
13	Daphnetin	124,300	5.13	$C_9H_6O_4$	179.034	179.0339	−0.1
14	Esculetin	124,300	5.13	$C_9H_6O_4$	179.034	179.0339	−0.1
15	Rutin	71,010	6.3	$C_{27}H_{30}O_{16}$	611.161	611.1621	2.3
16	Hyperin	297,200	6.5	$C_{21}H_{20}O_{12}$	465.103	465.1034	1.4
17	Isoscopoletin	42,290	6.69	$C_{10}H_8O_4$	193.05	193.0498	1.6
18	Isoferulic acid	2,997	6.74	$C_{10}H_{10}O_4$	195.065	195.0657	2.4
19	Luteoloside	1,829	6.96	$C_{21}H_{20}O_{11}$	449.108	449.1097	4.1
20	Narirutin	15,920	7.08	$C_{27}H_{32}O_{14}$	581.186	581.1875	1.8
21	Luteolin	107,100	7.14	$C_{15}H_{10}O_6$	287.055	287.0553	1
22	Genistein	31,520	7.38	$C_{21}H_{20}O_{10}$	433.113	433.1134	1
23	Hesperidin	55,530	7.48	$C_{28}H_{34}O_{15}$	611.197	611.1975	0.7
24	Pratensein-7-*O*-glucoside	4,385	7.7	$C_{22}H_{22}O_{11}$	463.123	463.1243	1.8
25	Tiliroside	190,600	8.91	$C_{30}H_{26}O_{13}$	595.145	595.1444	−0.4
26	Calycosin-7-*O*-glucoside	42,280	9.42	$C_{22}H_{22}O_{10}$	447.129	447.1293	1.5
27	Farrerol	249,800	10.35	$C_{17}H_{16}O_5$	301.107	301.1068	−0.8
28	Patchouli alcohol	611,500	12.24	$C_{15}H_{24}$	205.195	205.1949	−0.7
29	Nobiletin	99,200	12.77	$C_{21}H_{22}O_8$	403.139	403.1389	0.3
30	Diosgenin	38,270	14.75	$C_{27}H_{42}O_3$	415.321	415.3208	0.2
31	Ruscogenin	6,144	14.83	$C_{27}H_{42}O_4$	431.316	431.3175	4.4
32	Ophiopogonanone C	41,460	15.1	$C_{20}H_{20}O_6$	357.133	357.1333	0
33	Liriopesides B	256,700	15.11	$C_{39}H_{62}O_{12}$	723.431	723.4309	−0.7

temperature was 280°C. The temperature program used was as follows: the column temperature was held at 70°C for 2 min, increased by 10°C to 200°C, increased by 5°C to 280°C and held there for 6 min. The ion source and quadrupole rod temperatures were 230 and 150°C, respectively. The column effluent was fully scanned in the mass range of 50–550 *m/z*. The data were subjected to feature extraction and preprocessed with the XCMS package in R software (version 4.0.5, https://www.r-project.org/) and then normalized and edited into a two-dimensional data matrix by Excel 2010 software; data included the retention time (RT), the mass-to-charge ratio, observations (samples), and peak intensity.

2.8 LC-MS analysis

LC-MS was performed using an ACQUITYTM UPLC-QTOF platform (Waters, Wexford, Ireland) with a Waters ACQUITY UPLC HSS T3 column (2.1 mm × 100 mm, 1.8 μm). The mobile phases consisted of 0.1% aqueous formic acid (v/v) (A) and acetonitrile (B), and were introduced under the following gradient elution conditions: 0% B at 0–1 min, 0–20% B at 1–2 min, 20–50% B at 2–12 min, 50–95% B at 12–15 min, and 95–100% B at 15–20 min. The flow rate was set at 0.35 mL/min, and the column temperature was maintained at 40°C. The injection volume was 6 μL. The electrospray ionization source was set in both ESI (+) and ESI (−) ionization modes. The parameters were set as follows: source and desolvation temperatures: 120 and 350°C, respectively; desolvation gas (N_2) flow: 600 L/h; capillary voltages: 1.4 kV for ESI (+) and 1.3 kV for ESI (−); sampling cone: 40 V for ESI (+) and 23 V for ESI (−); cone gas (N_2) flow: 50 L/h; collision energy: 10–40 V; ion energy: 1 V; scan time: 0.03 s; and interscan time: 0.02 s. The mass range scanned was 50–1,500 *m/z*. MS data were collected with MassLynx 4.1 software.

Table 4: Putative identification of ZMD in negative ion mode

No.	Component name	Area	RT	Formula	Precursor mass	Found at mass	Mass error (ppm)
1	Histidine	11,660	1.08	$C_6H_9N_3O_2$	154.062	154.0622	−0.1
2	Arginine	165,500	1.09	$C_6H_{14}N_4O_2$	173.104	173.1044	0.1
3	D-(+)-Mannose	376,700	1.19	$C_6H_{12}O_6$	179.056	179.056	−0.8
4	L-Malic acid	2,191,000	1.35	$C_4H_6O_5$	133.014	133.0143	0.2
5	Fungitetraose	329,200	1.79	$C_{24}H_{42}O_{21}$	665.215	665.2146	0
6	Citric acid	7,804,000	1.94	$C_6H_8O_7$	191.02	191.0196	−0.5
7	Succinic acid	21,110	2.31	$C_4H_6O_4$	117.019	117.0192	−0.9
8	Adenine	10,630	2.37	$C_5H_5N_5$	134.047	134.0473	0.3
9	Guanosine	115,800	2.48	$C_{10}H_{13}N_5O_5$	282.084	282.0845	0.3
10	Gallic acid	54,280	2.66	$C_7H_6O_5$	169.014	169.0142	0
11	Phenylalanine	70,380	3.19	$C_9H_{11}NO_2$	164.072	164.0718	0.8
12	Vanillic acid	228,400	3.37	$C_8H_8O_4$	167.035	167.035	0.3
13	Hydroxytyrosol	11690	3.69	$C_8H_{10}O_3$	153.056	153.0559	1
14	L-Tryptophan	250,300	4.16	$C_{11}H_{12}N_2O_2$	203.083	203.0826	0.1
15	Salidroside	31,980	4.17	$C_{14}H_{20}O_7$	299.114	299.1138	0.7
16	4-Hydroxybenzoic acid	92,120	4.63	$C_7H_6O_3$	137.024	137.0244	0.1
17	4-*O*-caffeoyl quinic acid	264,700	4.8	$C_{16}H_{18}O_9$	353.088	353.0879	0.1
18	Esculetin	430,000	5.14	$C_9H_6O_4$	177.019	177.0193	−0.3
19	Caffeic acid	309,100	5.21	$C_9H_8O_4$	179.035	179.0348	−0.8
20	Eleutheroside E	14,750	5.88	$C_{34}H_{46}O_{18}$	787.267	787.2658	−1
21	Rutin	202,800	6.3	$C_{27}H_{30}O_{16}$	609.146	609.1456	−0.9
22	Hyperin	2,004,000	6.51	$C_{21}H_{20}O_{12}$	463.088	463.0879	−0.7
23	Astragalin	12,120	6.96	$C_{21}H_{20}O_{11}$	447.093	447.0931	−0.4
24	Specnuezhenide	872,500	7.04	$C_{31}H_{42}O_{17}$	685.235	685.2342	−1
25	Narirutin	43,210	7.08	$C_{27}H_{32}O_{14}$	579.172	579.1709	−1.8
26	Dicaffeoylquinic acid	34,110	7.49	$C_{25}H_{24}O_{12}$	515.119	515.1189	−1.2
27	Hesperidin	161,500	7.49	$C_{28}H_{34}O_{15}$	609.182	609.1816	−1.5
28	Quercetin	16,350	9.1	$C_{15}H_{10}O_7$	301.035	301.035	−1.3
29	Calycosin-7-*o*-glucoside	20,440	9.43	$C_{22}H_{22}O_{10}$	491.119	491.1178	−3.5
30	Apigenin	6,976	10.1	$C_{15}H_{10}O_5$	269.046	269.0448	−2.9
31	Butylparaben	2,508	13.24	$C_{11}H_{14}O_3$	193.087	193.0869	−0.7
32	Liriope muscari baily saponins C	5,340	13.53	$C_{44}H_{70}O_{17}$	869.454	869.4516	−2.8
33	Asiatic acid	31,510	14.06	$C_{30}H_{48}O_5$	487.343	487.3414	−3
34	Methylophiopogonone A	264,600	14.71	$C_{19}H_{16}O_6$	339.087	339.0865	−2.7
35	Ophiopogonin D	47,450	14.83	$C_{44}H_{70}O_{16}$	899.465	899.463	−1.7
36	Gingerglycolipid B	5,698	15.21	$C_{33}H_{58}O_{14}$	723.381	723.3777	−4.3
37	Corosolic acid	13,550	15.55	$C_{30}H_{48}O_4$	471.348	471.3464	−3.3
38	Ophiopogonanone C	201,100	15.72	$C_{19}H_{16}O_7$	355.082	355.0815	−2.2
39	Oleanolic acid	20,510	16.77	$C_{30}H_{48}O_3$	455.353	455.3524	−1.4

2.9 Data analysis

For UPLC-Q/TOF-MS analysis, the data were processed using SCIEX OS software with multiple confidence criteria, including quality accuracy, RT, isotopes, and matching use of compound libraries. In this study, the TCM MS/MS Library, which contains secondary data for more than 1,500 Chinese herbal medicines, was used to identify the target constituents based on the first-order accurate mass number, isotope distribution ratio, and MS/MS of the compounds. For GC-MS analysis, a total of 1,060 features were collected in this experiment, and the data were imported into SIMCA-P (version 13.0, Umetrics AB, Sweden) software for PCA and OPLS-DA. For LC-MS analysis, the data were first transformed to CDF files by CDFbridge and input into the XCMS package in R software and then normalized and edited into a two-dimensional data matrix by Excel 2007 software. A total of 1,712 features in ESI (+) ionization mode and 1,138 features in ESI (−) ionization mode were collected in this experiment, and the data were imported into SIMCA-P software to perform PCA and OPLS-DA.

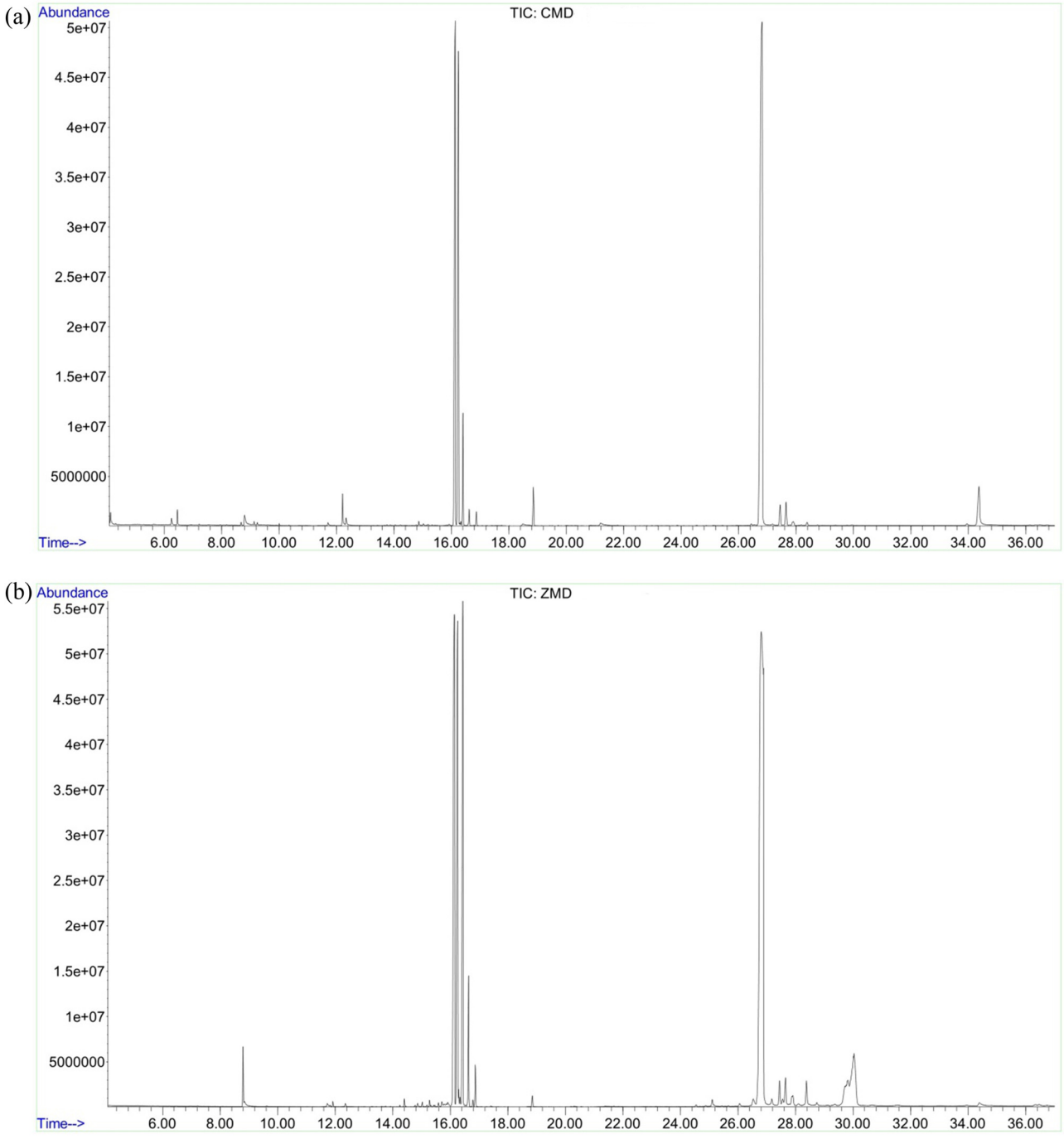

Figure 3: GC-MS chromatographs of CMD extract (a) and ZMD extract (b).

3 Results

3.1 UPLC/Q-TOF MS analysis of chemical constituents of CMD and ZMD

By using UPLC/Q-TOF MS analysis, CMD and ZMD could be analyzed within 21 min and exhibited some major peaks in the total ion chromatography, as shown in Figures 1 and 2, respectively. According to the TCM MS/MS Library in SCIEX OS software, the chemical constituents were identified qualitatively. As a result, a total of 26 chemical constituents of CMD were identified in positive ion mode and 33 chemical constituents of CMD were identified in negative ion mode in UPLC/Q-TOF MS analysis. Furthermore, a total of 33 chemical constituents of ZMD

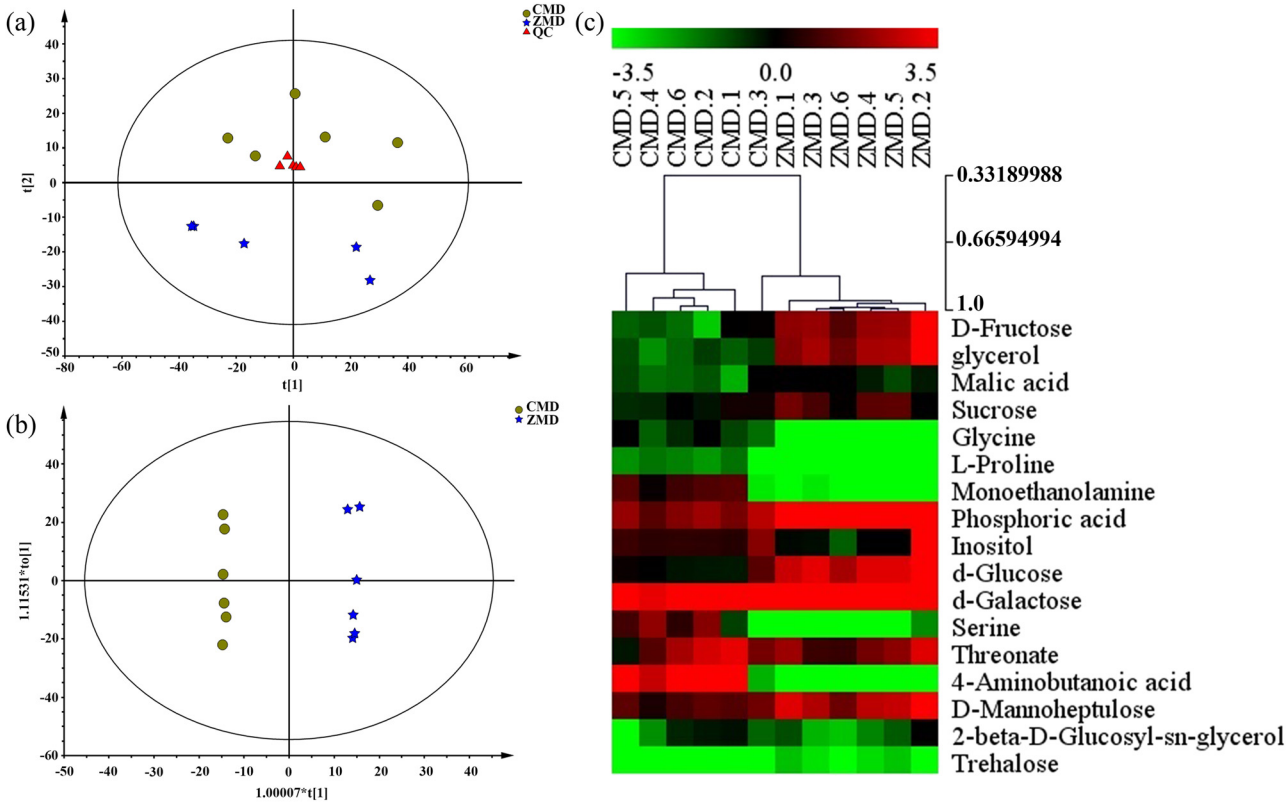

Figure 4: Multivariate statistical analysis of CMD and ZMD samples using GC-MS analysis: (a) PCA score plots for CMD, ZMD, and QC samples, (b) OPLS-DA score plots for CMD and ZMD, and (c) heatmap plot for the different chemical constituents of CMD and ZMD.

were identified in positive ion mode and 39 chemical constituents of ZMD were identified in negative ion mode in UPLC/Q-TOF MS analysis. Most of these chemical constituents were steroidal saponins, amino acids, homoisoflavonoids, polysaccharides, and nucleosides. Additionally, our UPLC/Q-TOF MS analysis revealed that the dried tubers of both CMD and ZMD contained methylophiopogonanone A, methylophiopogonanone B, methylophiopogonone A, ophiopogonin D, ophiopogonin D′, ophiopogonanone C, ophiopogonanone E, and ruscogenin. Detailed information on the identified chemical constituents is listed in Tables 1–4. Also, the MS fragmentation pathways for different chemical constituents of CMD and ZMD in positive ion mode or negative ion mode are shown in Tables S1 and S2, respectively.

3.2 GC-MS analysis of chemical constituents of CMD and ZMD

The total ion chromatograms of CMD and ZMD are shown in Figure 3. PCA and OPLS-DA were used to realize the CMD and ZMD clusters. In addition, the PCA score plot exhibited a relatively tight clustering of the QC samples, which confirmed the reliability of the MS data. As shown in Figure 4a, the CMD and ZMD groups were clearly separated in the PCA score plot ($R^2X = 0.864$, $Q^2 = 0.651$) with four PCs. Meanwhile, an OPLS-DA model was established ($R^2X = 0.912$, $R^2Y = 0.998$, and $Q^2 = 0.936$) and showed clear discrimination between CMD and ZMD groups (Figure 4b). A heatmap plot was generated to further characterize the significant differences. Variables with variable importance in the projection (VIP) values larger than 1 were considered to be potential chemical constituents, and 17 chemical constituents were selected (Figure 4c and Table S3).

3.3 Pathway enrichment of different chemical constituents in GC-MS analysis

To explore the roles of different chemical constituents based on GC-MS analysis, the different chemical constituents were imported into MetaboAnalyst 5.0 (https://www.metaboanalyst.ca/), a comprehensive platform dedicated to metabolomics data analysis via a user-friendly, web-based interface [14]. The impact value threshold was set to 0.1, and pathways with an impact value greater than the threshold were considered potential target pathways. As

Table 5: Pathways of significantly different chemical constituents in GC-MS analysis

No.	Pathway name	Metabolite	KEGG ID
1	Galactose metabolism	Glycerol	C00116
		D-Galactose	C00124
		D-Glucose	C00031
		Sucrose	C00089
2	Starch and sucrose metabolism	Trehalose	C01083
		beta-D-Fructose	C02336
		D-Glucose	C00031
		Sucrose	C00089
3	Cyanoamino acid metabolism	Glycine	C00037
		L-Serine	C00065
4	Methane metabolism	Glycine	C00037
		L-Serine	C00065
5	Aminoacyl-tRNA biosynthesis	Glycine	C00037
		L-Serine	C00065
		L-Proline	C00148
6	Glycine, serine, and threonine metabolism	L-Serine	C00065
		Glycine	C00037
7	Arginine and proline metabolism	Gamma-aminobutyric acid	C00334
		L-Proline	C00148
8	Amino sugar and nucleotide sugar metabolism	D-Galactose	C00124
		beta-D-Fructose	C02336
9	Sulfur metabolism	L-Serine	C00065
10	Glycerolipid metabolism	Glycerol	C00116
11	Sphingolipid metabolism	L-Serine	C00065
12	Nitrogen metabolism	Glycine	C00037
13	Glyoxylate and dicarboxylate metabolism	L-Malic acid	C00149
14	Butanoate metabolism	Gamma-aminobutyric acid	C00334
15	Citrate cycle (TCA cycle)	L-Malic acid	C00149
16	Carbon fixation in photosynthetic organisms	L-Malic acid	C00149
17	Pyruvate metabolism	L-Malic acid	C00149
18	Alanine, aspartate, and glutamate metabolism	Gamma-aminobutyric acid	C00334
19	Glycerophospholipid metabolism	Ethanolamine	C00189
20	Glutathione metabolism	Glycine	C00037
21	Cysteine and methionine metabolism	L-Serine	C00065

shown in Table 5, the therapeutic effect of CMD and ZMD was probably associated with galactose metabolism; starch and sucrose metabolism; cyanoamino acid metabolism; methane metabolism; aminoacyl-tRNA biosynthesis; glycine, serine, and threonine metabolism; arginine and proline metabolism; amino sugar and nucleotide sugar metabolism; sulfur metabolism; and glycerolipid metabolism (Table 5).

3.4 LC-MS analysis of chemical constituents of CMD and ZMD

The CMD and ZMD extracts were also analyzed by LC-MS in both positive and negative ion modes. The base peak chromatograms of LC-MS are shown in Figure 5a and b. As shown in Figure 6a, the CMD and ZMD groups were also clearly separated in the PCA score plot (R^2X = 0.59, Q^2 = 0.303) with three PCs. Then, the OPLS-DA model was established (R^2X = 0.658, R^2Y = 1, and Q^2 = 0.892) in positive ion mode (Figure 6c). And, an OPLS-DA model was established (R^2X = 0.763, R^2Y = 1, and Q^2 = 0.93) in negative ion mode (Figure 6d), and both showed clear discrimination of the CMD and ZMD groups in negative ion mode (R^2X = 0.63, Q^2 = 0.279; Figure 6b) with three PCs. Furthermore, we found 25 differences in the chemical constituents of CMD and ZMD in positive ion mode (Figure 7a and Table S4) and a total of 17 differences in the chemical constituents of CMD and ZMD in negative ion mode (Figure 7b and Table S5).

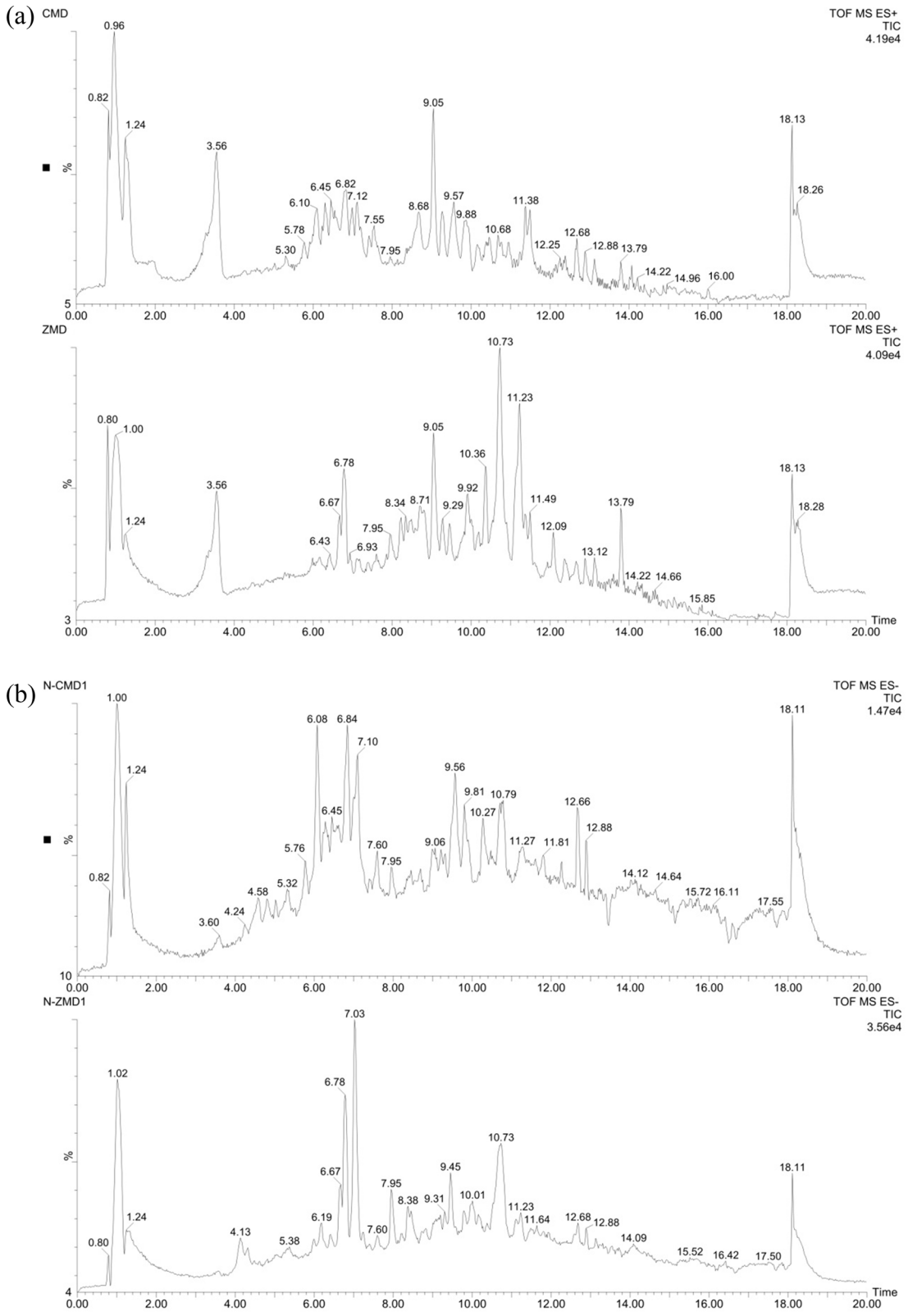

Figure 5: Base peak chromatograms of CMD and ZMD obtained by LC-MS in positive mode (a) and negative mode (b).

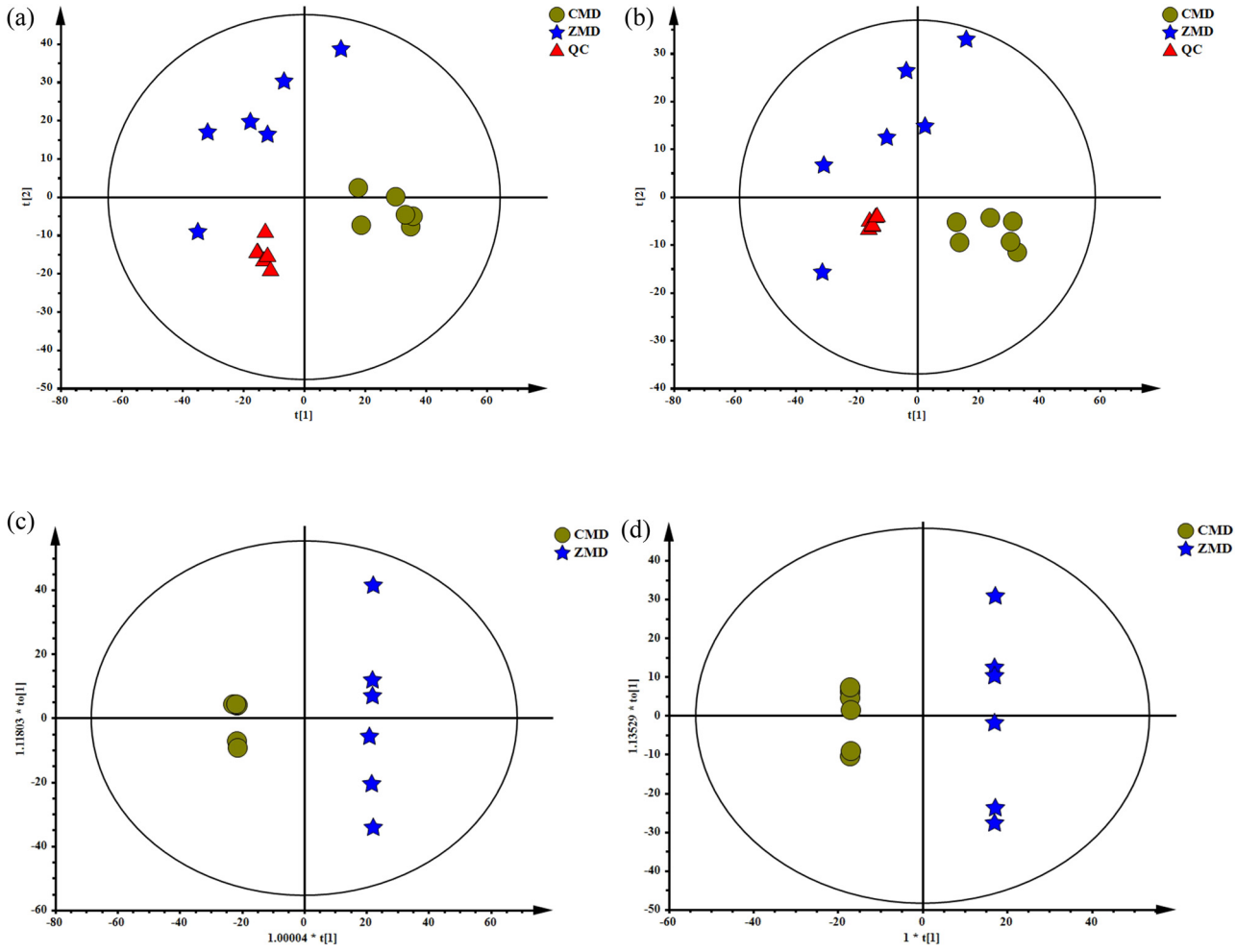

Figure 6: PCA and OPLS-DA score plots of CMD and ZMD samples in (a and c) positive ion mode and (b and d) negative ion mode.

3.5 Pathway enrichment of different chemical constituents in LC-MS analysis

Similarly, metabolic pathways of different chemical constituents were analyzed in LC-MS analysis using the integrated web-based tool MetaboAnalyst. In our study, the 25 different chemical constituents between CMD and ZMD in the positive ion mode were mainly associated with tropane, piperidine, and pyridine alkaloid biosynthesis; sulfur metabolism; stilbenoid, diarylheptanoid, and gingerol biosynthesis; and cysteine and methionine metabolism (Table 6). Moreover, the 17 differences in the chemical constituents of CMD and ZMD in the negative ion mode were related to valine, leucine, and isoleucine biosynthesis; diterpenoid biosynthesis; pantothenate and CoA biosynthesis; flavonoid biosynthesis; glycolysis or gluconeogenesis; carbon fixation in photosynthetic organisms; and glycerophospholipid metabolism (Table 7). These data suggested that there were many differences between CMD and ZMD. Additionally, CMD and ZMD likely act to nourish yin through all three signaling pathways.

4 Discussion

The tubers of Ophiopogonis Radix (Maidong in Chinese) are an important Chinese herb and functional health food. However, the quality of CMD and ZMD remains to be distinguished and evaluated. In this respect, UPLC-Q/TOF-MS provides accurate structural information about bioactive compounds for the identification of TCM [15]. In addition, metabolomics provides new insights into understanding global metabolic changes and the multiple related biochemical pathways of altered metabolites [16,17]. GC-MS and LC-MS have become two of the most commonly used high-throughput technologies in metabolomics research due to their high sensitivity and favorable reproducibility [16,18,19].

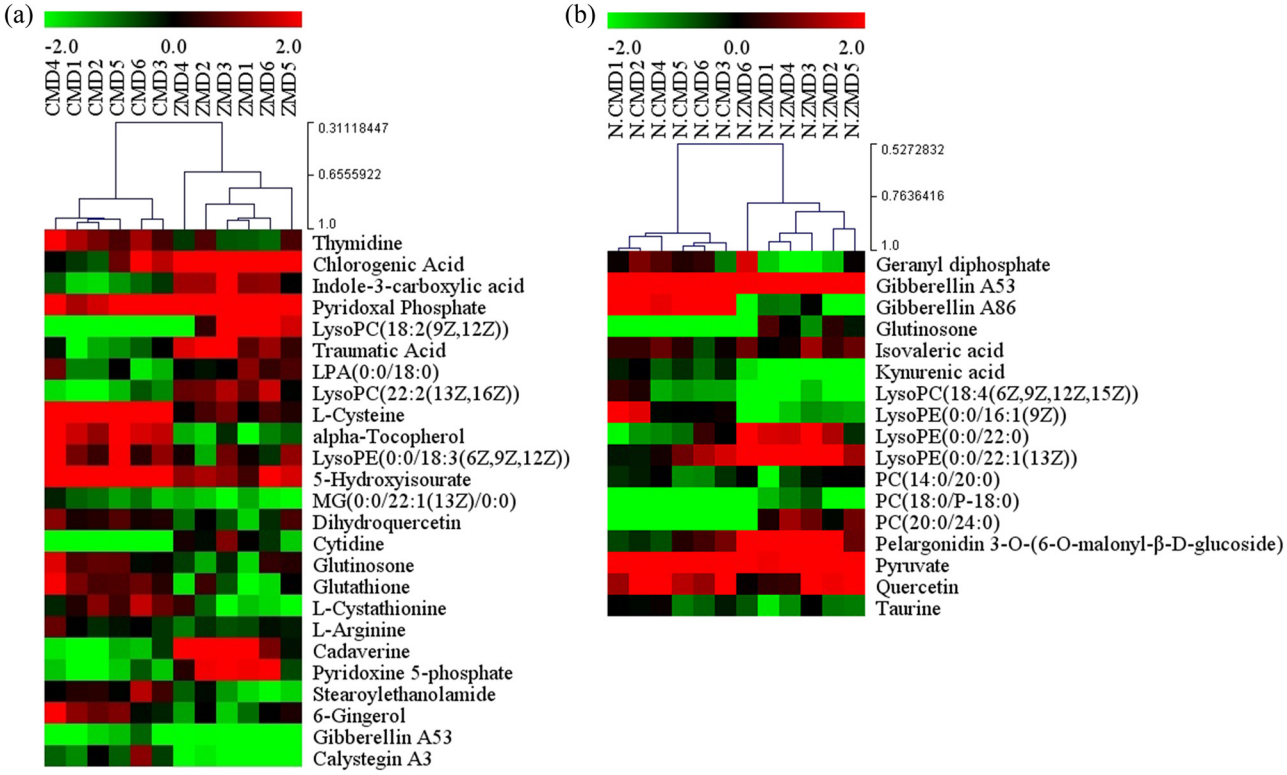

Figure 7: Heatmap plot for the different chemical constituents between CMD and ZMD using LC-MS analysis in (a) positive ion mode and (b) negative ion mode.

Table 6: Pathways of significantly different chemical constituents (ESI+)

No.	Pathway name	Metabolite	KEGG ID
1	Tropane, piperidine, and pyridine alkaloid biosynthesis	Cadaverine	C01672
2	Sulfur metabolism	L-Cysteine	C00097
3	Stilbenoid, diarylheptanoid, and gingerol biosynthesis	Chlorogenic acid	C00852
4	Cysteine and methionine metabolism	L-Cysteine	C00097
		L-Cystathionine	C02291
5	Glycerophospholipid metabolism	Phosphatidate	C00416
		2-Lysophosphatidylcholine	C04230
6	Phenylpropanoid biosynthesis	Chlorogenic acid	C00852
7	Diterpenoid biosynthesis	Gibberellin A53	C06094
8	Arginine and proline metabolism	L-Arginine	C00062
9	Thiamine metabolism	L-Cysteine	C00097
10	Aminoacyl-tRNA biosynthesis	L-Arginine	C00062
		L-Cysteine	C00097
11	Flavonoid biosynthesis	Taxifolin	C01617
		Chlorogenic acid	C00852
12	Purine metabolism	5-Hydroxyisourate	C11821
13	Glutathione metabolism	L-Cysteine	C00097
		Cadaverine	C01672
		Glutathione	C00051
14	Glycerolipid metabolism	Phosphatidate	C00416
15	Pyrimidine metabolism	Cytidine	C00475
		Thymidine	C00214
16	Ubiquinone and other terpenoid-quinone biosynthesis	Alpha-tocopherol	C02477
17	Vitamin B6 metabolism	Pyridoxal 5′-phosphate	C00018
		Pyridoxine 5′-phosphate	C00627

Table 7: Pathways of significantly different chemical constituents (ESI−)

No.	Pathway name	Metabolite	KEGG ID
1	Valine, leucine, and isoleucine biosynthesis	Pyruvic acid	C00022
2	Butanoate metabolism	Pyruvic acid	C00022
3	Pyruvate metabolism	Pyruvic acid	C00022
4	Diterpenoid biosynthesis	Gibberellin A53	C06094
5	Pantothenate and CoA biosynthesis	Pyruvic acid	C00022
6	Flavonoid biosynthesis	Quercetin	C00389
7	Glycolysis or gluconeogenesis	Pyruvic acid	C00022
8	Carbon fixation in photosynthetic organisms	Pyruvic acid	C00022
9	Glycerophospholipid metabolism	2-Lysophosphatidylcholine	C04230
		Phosphatidylcholine	C00157
10	Alanine, aspartate, and glutamate metabolism	Pyruvic acid	C00022
11	Citrate cycle (TCA cycle)	Pyruvic acid	C00022
12	C5-branched dibasic acid metabolism	Pyruvic acid	C00022
13	Terpenoid backbone biosynthesis	Pyruvic acid	C00022
		Geranyl-PP	C00341
14	Flavone and flavonol biosynthesis	Quercetin	C00389
15	Glycine, serine, and threonine metabolism	Pyruvic acid	C00022
16	Monoterpenoid biosynthesis	Geranyl-PP	C00341
17	Taurine and hypotaurine metabolism	Taurine	C00245
18	Cysteine and methionine metabolism	Pyruvic acid	C00022

Due to the complexity of chemical components in MD, it is difficult for traditional methods to thoroughly isolate trace ingredients with a single method. Therefore, multiple analytical platforms are needed.

In this study, efficient and reliable methods based on UPLC-Q/TOF-MS, GC-MS, and LC-MS analyses were used to identify the bioactive chemical constituents in CMD and ZMD. For UPLC-Q/TOF-MS analysis, UPLC-Q/TOF-MS technology has greatly improved the speed of analysis and detection in plants [20]. Overall, a total of 59 and 72 chemical constituents were quickly identified in CMD and ZMD, respectively, including steroidal saponins, homoisoflavonoids, amino acids, and nucleosides. Among them, isoleucine, chlorogenic acid, daphnetin, rutin, isoscopoletin, luteolin, genistein, hesperidin, pratense-7-*O*-glucoside, farrerol, patchouli alcohol, diosgenin, arginine, fungitetraose, adenine, hydroxytyrosol, salidroside, eleutheroside E, astragalin, specnuezhenide, dicaffeoylquinic acid, quercetin, apigenin, butylparaben, asiatic acid, and oleanolic acid existed only in ZMD, while glutamic acid, betaine, cinnamic acid, syringaldehyde, neohesperidin, leucine, shikimic acid, ellagic acid, gracillin, and methylophiopogonanone B existed only in CMD. In general, these results showed that there were many differences between the bioactive chemical constituents of Ophiopogonis Radix from different production areas.

Metabolomics can help to assess the physiological state of an organism in diverse biochemical events [21]. Previously, Lyu et al. reported that *O. japonicas* from Zhejiang and Sichuan can clearly be separated by using UPLC/Q-TOF MS-based metabolome analysis where CMD showed higher level steroidal saponins, and ZMD had higher contents of homoisoflavonoids specifically [20]. Similarly,i this study, for GC-MS and LC-MS-based metabolome analyses, the PCA results showed that the CMD and ZMD samples were divided into two clusters and indicated that metabolite profiling by GC-MS and LC-MS also contributes to discriminating CMD and ZMD samples from different geographical origins. Moreover, the OPLDA and VIP values revealed that the bioactive chemical constituents in CMD and ZMD were significantly different. Among them, 4-aminobutanoic acid, glycine, L-proline, monoethanolamine, and serine showed higher levels in CMD according to the results of GC-MS analysis. In addition, the contents of chlorogenic acid, traumatic acid, cytidine, cadaverine, pyridoxine 5-phosphate, glutinone, and pelargonidin 3-*O*-(6-*O*-malonyl-β-D-glucoside) were remarkably higher than those in CMD. Moreover, these different constituents were mainly associated with multiple metabolic pathways, such as galactose metabolism; starch and sucrose metabolism; cysteine and methionine metabolism; valine, leucine, and isoleucine biosynthesis; and glycerophospholipid metabolism. Significantly, galactose is crucial for human metabolism, with an established role in energy delivery and the galactosylation of complex molecules [22]. Additionally, sucrose plays a central role in

the control of carbon flux in the biosynthesis of different storage reserves [23]. Xu et al. showed that methionine restriction, a dietary regimen that protects against metabolic diseases and aging, represses cancer growth and improves cancer therapy [24]. Interestingly, leucine and isoleucine reduced body weight and white adipose tissue weight by regulating lipid metabolism-related genes in high-fat diet-induced obese mice [25]. Overall, the bioactive chemical constituents in CMD and ZMD are involved in diverse metabolic pathways with different pharmacological effects. However, there are some limitations to this study. The number of samples is too small to be representative for multivariate statistical analysis. The sample size should be expanded for further study. In further research, we will focus on the molecular mechanisms of different chemical constituents in Maidong, which are critical for developing Maidong for pharmacology and clinical uses.

5 Conclusion

In summary, UPLC-Q/TOF-MS, GC-MS, and LC-MS analyses combined with multivariate statistical analysis could provide basic information for the discrimination and quality evaluation of Ophiopogonis Radix from two different production areas. These findings suggested that the ZMD samples showed higher levels of one type of bioactive chemical constituent than the CMD samples, demonstrating that the geographical area influenced the accumulation of bioactive constituents. This study also lays foundations for future studies on the quantitative analysis of the 12 bioactive chemical constituents between CMD and ZMD and their relevant metabolic pathways, which will contribute to increasing the understanding of the pharmacodynamic effects and improve the development of Ophiopogonis Radix in TCM.

Acknowledgments: This study was completed in the Ningbo College of Health Science. We would like to thank the teachers at this college for their guidance.

Funding information: This work was financially supported by the National Natural Science Foundations of Ningbo (No. 2019C50082 and No. 202002N3172) and the "2025" Major Science and Technology Project of Ningbo (No. 2019B10008).

Author contributions: G.W.L. and Q.X. conceived and supervised the study; G.W.L. designed the experiments; G.W.L., X.Y.Z., Q.C., and L.Z. performed the experiments; G.W.L. and L.Z. analyzed the data and wrote the manuscript. All authors reviewed the results and approved the final version of the manuscript.

Conflict of interest: Authors state no conflict of interest.

Data availability statement: The datasets generated during and/or analyzed during the current study are available from the corresponding author on reasonable request.

References

[1] Wang M, Hou X, Wang H. Genomic sequence resource of alternaria alternata strain B3 causing leaf blight on *Ophiopogon japonicus*. Plant Dis. 2021;105(3):684–7.
[2] He J, Ye L, Li J, Huang W, Huo Y, Gao J, et al. Identification of ophiopogonis radix from different producing areas by headspace-gas chromatography-ion mobility spectrometry analysis. J Food Biochem. 2021;46:e13850.
[3] Wang Y, Zhou X, Chen X, Wang F, Zhu W, Yan D, et al. Efficacy and safety of shengmai injection for chronic heart failure: a systematic review of randomized controlled trials. Evid Based Complement Alternat Med. 2020;2020:9571627.
[4] Mao D, Tian XY, Mao D, Hung SW, Wang CC, Lau CBS, et al. A polysaccharide extract from the medicinal plant maidong inhibits the IKK-NF-κB pathway and IL-1β-induced islet inflammation and increases insulin secretion. J Biol Chem. 2020;295(36):12573–87.
[5] Yang Y, Zhou Y. Shashen-maidong decoction-mediated IFN-γ and IL-4 on the regulation of Th1/Th2 imbalance in RP rats. Biomed Res Int. 2019;2019:6012473.
[6] Yang L, Zhang C, Chen J, Zhang S, Pan G, Xin Y, et al. Shenmai injection suppresses multidrug resistance in MCF-7/ADR cells through the MAPK/NF-κB signalling pathway. Pharm Biol. 2020;58(1):276–85.
[7] Wang L, Zhou Y, Qin Y, Wang Y, Liu B, Fang R, et al. Methylophiopogonanone B of radix ophiopogonis protects cells from H_2O_2-induced apoptosis through the NADPH oxidase pathway in HUVECs. Mol Med Rep. 2019;20(4):3691–700.
[8] Zhang HQ, Liu P, Duan JA, Dong L, Shang EX, Qian DW, et al. Comparative analysis of carbohydrates, nucleosides and amino acids in different parts of *Trichosanthes kirilowii* maxim. by (ultra) high-performance liquid chromatography coupled with tandem mass spectrometry and evaporative light scattering detector methods. Molecules. 2019;24(7):1440.
[9] Zhou P, Gao G, Zhao CC, Li JY, Peng JF, Wang SS, et al. In vivo and in vitro protective effects of shengmai injection against doxorubicin-induced cardiotoxicity. Pharm Biol. 2022;60(1):638–51.
[10] Tan M, Chen J, Wang C, Zou L, Chen S, Shi J, et al. Quality evaluation of Ophiopogonis Radix from two different producing areas. Molecules. 2019;24(18):3220.
[11] Yu K, Liu W, Zhang N, Cheng X, Zhou S, Zuo T, et al. A novel method to identify three quality grades of herbal medicine Ophiopogonis Radix by microscopic quantification. Front Pharmacol. 2021;11:591310.

[12] Luo H, Ming LS, Tong TT, Tang Y, Yang J, Shen L, et al. Chemical comparison of Ophiopogonis Radix and Liriopes Radix based on quantitative analysis of multiple components by HPLC coupled with electrospray ionization tandem triple quadrupole mass spectrometry. J AOAC Int. 2020;103(4):1148–59.
[13] Tian Y, Gong P, Wu Y, Chang S, Xu J, Yu B, et al. Screening and identification of potential active components in Ophiopogonis Radix against atherosclerosis by biospecific cell extraction. J Chromatogr B Analyt Technol Biomed Life Sci. 2019;1133:121817.
[14] Pang Z, Chong J, Li S, Xia J. MetaboanalystR 3.0: toward an optimized workflow for global metabolomics. Metabolites. 2020;10(5):186.
[15] Ma F, Cui Q, Bai G. Combining UPLC/Q-TOF-MS/MS with biological evaluation for NF-κB inhibitors in uyghur medicine althaea rosea flowers. Front Plant Sci. 2019;9:1975.
[16] Shao C, Lu W, Hao H, Ye H. Functional metabolomics and chemoproteomics approaches reveal novel metabolic targets for anticancer therapy. Adv Exp Med Biol. 2021;1280:131–47.
[17] Zhang H, Zhang S, Wang W, Wang Q, Kuang H, Wang Q. Characterizing metabolites and potential metabolic pathways changes to understanding the mechanism of medicinal plant Phellodendri Amurensis cortex against doxorubicin-induced nephritis rats using UPLC-Q/TOF-MS metabolomics. J Pharm Biomed Anal. 2020;188:113336.
[18] Kibi M, Nishiumi S, Kobayashi T, Kodama Y, Yoshida M. GC/MS and LC/MS-based tissue metabolomic analysis detected increased levels of antioxidant metabolites in colorectal cancer. Kobe J Med Sci. 2019;65(1):E19–27.
[19] Feussner K, Feussner I. Comprehensive LC-MS-based metabolite fingerprinting approach for plant and fungal-derived samples. Methods Mol Biol. 2019;1978:167–85.
[20] Lyu CG, Kang CZ, Kang LP, Yang J, Wang S, He YL, et al. Structural characterization and discrimination of *Ophiopogon japonicas* (Liliaceae) from different geographical origins based on metabolite profiling analysis. J Pharm Biomed Anal. 2020;185:113212.
[21] Slaveykova VI, Majumdar S, Regier N, Li W, Keller AA. Metabolomic responses of green alga *Chlamydomonas reinhardtii* exposed to sublethal concentrations of inorganic and methylmercury. Environ Sci Technol. 2021;55(6):3876–87.
[22] Conte F, van Buuringen N, Voermans NC, Lefeber DJ. Galactose in human metabolism, glycosylation and congenital metabolic diseases: time for a closer look. Biochim Biophys Acta Gen Subj. 2021;1865(8):129898.
[23] Xu Q, Yin S, Ma Y, Song M, Song Y, Mu S, et al. Carbon export from leaves is controlled via ubiquitination and phosphorylation of sucrose transporter SUC2. Proc Natl Acad Sci U S A. 2020;117(11):6223–30.
[24] Xu Q, Li Y, Gao X, Kang K, Williams JG, Tong L, et al. HNF4α regulates sulfur amino acid metabolism and confers sensitivity to methionine restriction in liver cancer. Nat Commun. 2020;11(1):3978.
[25] Ma Q, Zhou X, Hu L, Chen J, Zhu J, Shan A. Leucine and isoleucine have similar effects on reducing lipid accumulation, improving insulin sensitivity and increasing the browning of WAT in high-fat diet-induced obese mice. Food Funct. 2020;11(3):2279–90.